

Research on Static Strength Design of Civil Aircraft Ceiling

Lu Liu*

Shanghai Aircraft Design and Research Institute, Shanghai, China

*Corresponding author's e-mail: liulu2@comac.cc

Abstract. The finite element analysis method is an important means to check the strength of civil aircraft interiors. In this paper, a typical structure of a civil aircraft interior is discussed, the analysis objects and loads are sorted out, the finite element model of the typical structure is established, and an engineering algorithm is proposed to check the fasteners. Taking the cabin ceiling of a civil aircraft as an example, it is proved that the proposed method has certain engineering application significance.

Keywords: Airframe Interior, Finite Element, Strength Analysis.

1 Introduction

The main cabin ceiling is mounted on the fuselage floor rail. The loads used for the main cabin ceiling body and its installation strength check to consider the fuselage overload envelope and fuselage static load in the case of aircraft dynamic load [1-8]. Overload envelope and emergency landing loads as specified in CCAR25.561, the safety factor of CCAR25.303, and the special factors of CCAR25.619 and 25.625 are considered. In this paper, the research parts are the main cabin ceiling body, the connection strength between the bodies, and the body's structure and the airframe.

The main cabin ceiling is mounted on the forward (FWD) fuselage floor rail. The top is connected to the C-shaped groove via four bolts, and the main cabin ceiling's body panel is constructed of honeycomb sandwich panels. The structure of the cabin ceiling is illustrated in Figure 1 below.

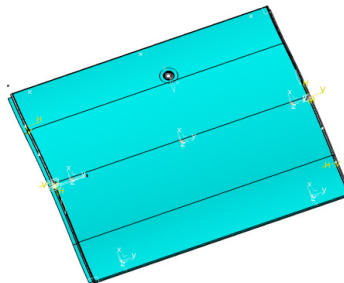


Fig. 1. The structure of the cabin ceiling.

2 Material and Fastener Performance

The materials used for the main cabin ceiling are listed in Tables 1 to 3. The mechanical property data of the fasteners employed are presented in Table 4.

Table 1. Performance of metal materials for main cabin ceiling.

Material grade	Mechanical properties				E (GPa)	μ
	σ _{tu} (MPa)		σ _{bru} (MPa)			
	A	B	A	B		
2024-T3511	414	427	661	682	72	0.33
2024-O-T42	414	427	661	682	72	0.33
304	517		1, 116		200	0.28

Table 2. Properties of main composite materials for main cabin ceiling (prepreg).

Material	Modulus of elasticity E11 (MPa)	Modulus of elasticity E22 (MPa)	Shear mod- ulus G12 (MPa)	Poisson's ratio μ_{12}	Single layer thickness (mm)	Shear strength L (MPa)	Shear strength W (MPa)
Prepreg	24, 000	24, 000	4, 500	0.07	0.250	30	30

Table 3. Properties of main composite materials for main cabin ceiling (prepreg).

Material	Modulus of compression E3 (MPa)	Compres- sive strength (MPa)	Shear mod- ulus LT G13 (MPa)	Shear mod- ulus WT G23 (MPa)	Shear strength LT (MPa)	Shear strength WT (MPa)
Honey- comb core	91.45	1.24	39	21	1.24	0.65
Honey- comb core	138	1.24	44	26	1.1	0.58

Table 4. Performance of metal materials for main cabin ceiling.

Type of fastener	Stretch allowable (N)	Shear allowable value (N)
Rivet	27, 545	20, 692 (single shear)
Rivet	1, 531	4, 828 (single shear)
Screw	11, 080	9, 456 (single shear)
Insert	1, 029	1, 854 (single shear)

3 Load

The design of the main cabin ceiling must comprehensively consider the dynamic load envelope, static load envelope, emergency landing load, and pressure relief load of A-

type aircraft [9]. Based on the aircraft's load envelope, the limiting overload coefficient for the corresponding station on the main cabin ceiling is derived. This coefficient is then multiplied by a safety factor of 1.5 to obtain the limit overload coefficient in each direction corresponding to the station where the main cabin ceiling is located. The maximum value of the limit overload in each direction under the aforementioned conditions is selected as the load for the corresponding station on the main cabin ceiling. The most severe limiting inertial load case is presented in Table 5.

Table 5. Selection of limit inertia load coefficient at the center of gravity of the main cabin ceiling.

Load case	Turn left	Right	Forward	Backwards	Up	Down
Emergency landing conditions	3	3	9	1.5	3	6
Static load case	0.76	0.76	2.05	1.66	1.5	5.33
Dynamic load case	0.41	0.41	-	-	1.3	7
The load factor	3	3	9	1.66	3	7

4 Establishment of Finite Element Model

The finite element model is established based on the structural elements and connections of the main cabin ceiling, with the body panel modeled using SHELL elements [10]. The joints of the main cabin ceiling constrain its linear displacement in all three directions. The finite element model of the main cabin ceiling, established as described above, is shown in Figure 2.

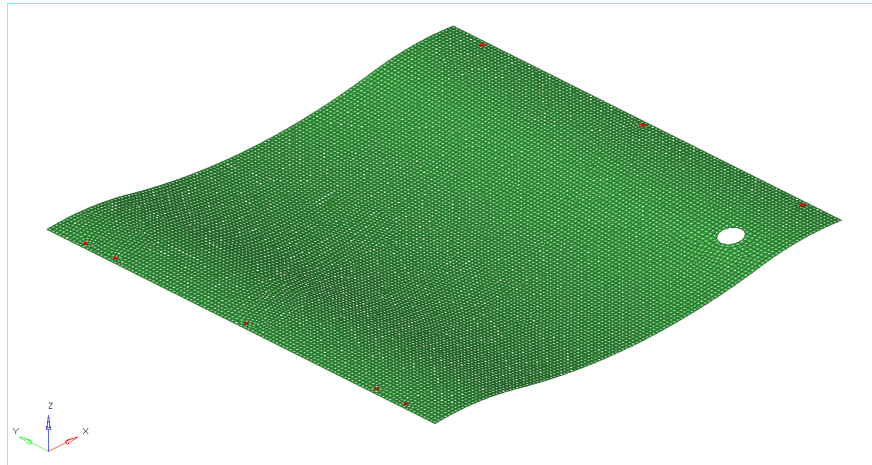


Fig. 2. The finite element model of the cabin ceiling.

5 Strength Analysis

5.1 Strength Analysis of Main Cabin Ceiling Body

According to the finite element results, under the pressure relief load condition, the maximum shear stress of the panel in the XY direction is $\tau_{XY} = 28.7MPa$, as shown in Figure 3. If the allowable shear stress of the panel is known $[\tau] = 30MPa$, the shear safety margin of the panel in the XY direction can be calculated as follows:

$$M.S. = \frac{[\tau]}{\tau_{XY}} - 1 = \frac{30}{28.7} - 1 = 0.05 \quad (1)$$

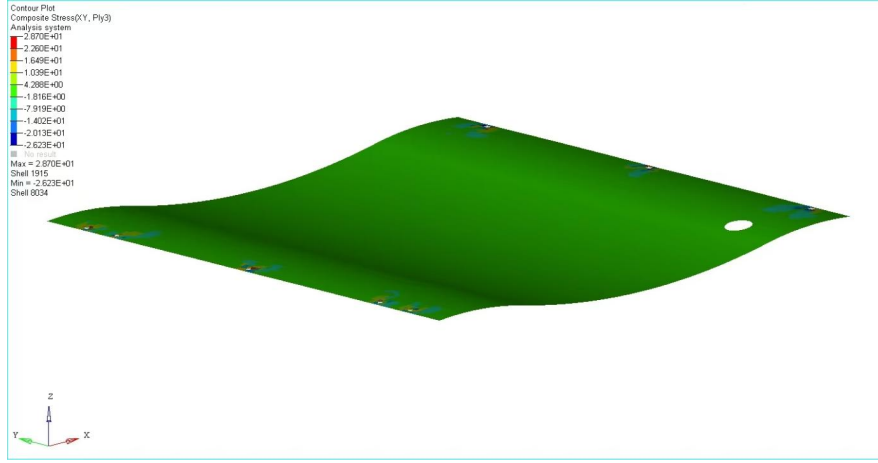


Fig. 3. The maximum shear stress of the panel in the XY.

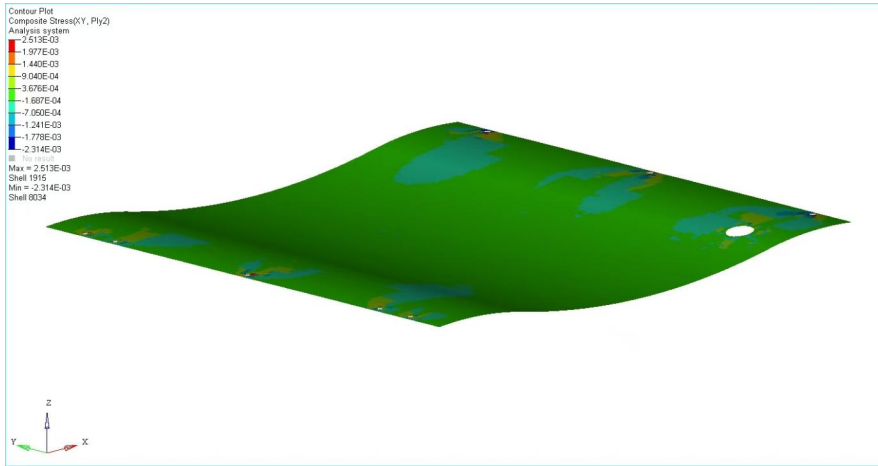


Fig. 4. The maximum shear stress of the honeycomb core in the XY.

According to the finite element results, under the pressure relief load condition, the maximum shear stress of the honeycomb core in the XY direction is $\tau_{XY} = 0.002MPa$, as shown in Figure 4. If the allowable shear stress of the panel is known $[\tau_{XY}] = 1.1MPa$, the shear safety margin of the panel in the XY direction can be calculated as follows:

$$M.S. = \frac{[\tau_{XY}]}{\tau_{XY}} - 1 = \frac{0.58}{0.005} - 1 = 115 \quad (2)$$

According to the finite element calculation results, the honeycomb core experiences the maximum compressive stress under the pressure relief working condition, and the maximum compressive stress is $\tau_{XY} = 0.002MPa$. The stress nephogram is shown in Figure 5, and the allowable stress for honeycomb core compression is $[\sigma_c] = 1.24MPa$. The compression safety margin of the honeycomb core is then calculated as:

$$M.S. = \frac{[\sigma_c]}{\sigma_c} - 1 = \frac{1.24}{0.002} - 1 = 619 \quad (3)$$

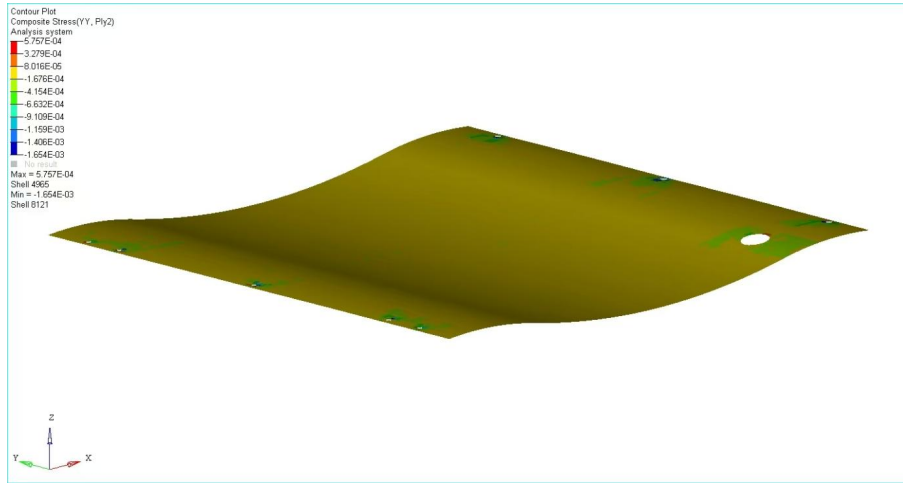


Fig. 5. The maximum compressive stress of the honeycomb core under the pressure relief working condition.

5.2 Main Cabin Ceiling Connection

C-shaped grooves are used to connect the ceiling panels of the main cabin, and the allowable stress of the material used for these grooves is $[\sigma_{tu}] = 414MPa$, as can be seen from the calculation results of the engineering algorithm. The connecting C-shaped groove between the panels of the main cabin ceiling experiences the maximum

working stress, and the maximum working stress is $\sigma = 295 \text{ MPa}$. Then, the safety margin of the connecting corner piece can be calculated as:

$$M.S. = \frac{[\sigma_{tu}]}{\sigma} - 1 = \frac{414}{295} - 1 = 0.40 \quad (4)$$

5.3 Connection Strength Check of the Main Cabin Ceiling

According to the calculation results of the engineering algorithm, under the pressure relief load condition, the connecting fasteners are subjected to the maximum tensile and shear loads, which are $F_t = 641 \text{ N}$ and $F_s = 419 \text{ N}$, respectively. Since the working load of the fastener is far less than its allowable load, the fastener meets the strength requirements. Under this load, the margin of safety for tension and shear of the blind hole insert can be calculated as follows:

$$M.S. = \frac{[F_t]}{F \times 1.15} - 1 = \frac{1043}{641 \times 1.15} - 1 = 0.41 \quad (5)$$

Shear allowance:

$$M.S. = \frac{[F_s]}{F_s \times 1.15} - 1 = \frac{2331}{419 \times 1.15} - 1 = 3.84 \quad (6)$$

The blind hole insert should be evaluated based on a tension-shear combination, and the tension-shear combination factor of safety (or allowance) should be determined as follows:

$$\begin{aligned} M.S. &= \frac{1}{1.15 \times \sqrt{\left(\frac{F_s}{[F_s]}\right)^2 + \left(\frac{F_t}{[F_t]}\right)^2}} - 1 \\ &= \frac{1}{1.15 \times \sqrt{\left(\frac{419}{1836}\right)^2 + \left(\frac{641}{1029}\right)^2}} - 1 \\ &= 0.31 \end{aligned} \quad (7)$$

6 Conclusion

In this paper, the strength of the ceiling of the main cabin under different working conditions is checked by means of finite element analysis and engineering algorithms. Taking the cabin interior of a civil aircraft as an example, the basic performance data of the connection that needs to be analyzed for some internal static strength analysis are obtained, and stored for subsequent structural design. This article only discusses the influence of static strength on ceiling structures. In the future, more factors that affect the strength of ceiling structures, such as temperature changes and vibration loads, will be

considered to provide a more comprehensive strength assessment. To fully understand the structural strength of civil aircraft interiors, additional research on theoretical calculation methods is required to explore the application of new materials or connection technologies in cabin ceiling structures, such as high-strength composite materials or advanced fastening systems, to enhance the overall strength and lightweight level of the structure.

References

1. B. C. Furtado A., et al. (2021). "A methodology to generate design allowable of composite laminates using machine learning--ScienceDirect". *International Journal of Solids and Structures*.
2. Pogosyan M., Nazarov E., Bolshikh A., et al. (2021). Aircraft composite structures integrated approach: a review [C]// *Journal of Physics: Conference Series*. IOP Publishing, 1925 (1): 012005.
3. Ardila Parra S. A., Pappalardo C. M., Estrada O. A. G., et al. (2020). Finite element-based redesign and optimization of aircraft structural components using composite materials [J]. *IAENG International Journal of Applied Mathematics*.
4. Cui L., Zeng Z., & Jiao S. (2024). Finite element analysis of eddy current testing of aluminum honeycomb sandwich structure with CFRP panels based on the domain decomposition method. *Journal of Nondestructive Evaluation* (2), 43.
5. WANG J., ZHANG X., and CHEN K. (2021). Study on thermo-mechanical coupling method of ship cabin with ceiling vent under fire condition [J]. *Chinese Journal of Ship Research*, 16 (3): 74-85.
6. Aircraft Design Manual's Editors 2001. Aircraft design manual: Vol. 9, load, strength, and stiffness [M]. Beijing: Aviation Industry Press (in Chinese).
7. Mauro G. D., Gagliardi G. M., Guida M., & Marulo F. (2023). Parachute emergency landing simulation and enhanced composite material characterization for general aviation aircraft. *Proceedings of the Institution of Mechanical Engineers, Part C: Journal of Mechanical Engineering Science*.
8. WAN C. H., DUAN S. H., NIE X. H., et al. (2018). Study on finite element modeling for large aircraft structures [J]. *Mechanical Science and Technology for Aerospace Engineering*, 37 (5): 816-820.
9. HE Zhiqun, LIU Yang, and LI Zhejiang (2019). Load design for full-scale static test of slat on large civil aircraft [J]. *ACTA AERONAUTICA ET ASTRONAUTICA SINICA*, 40 (2): 522, 197-522, 197.
10. Santare M. H. & Lambros J. (2000). Use of graded finite elements to model the behavior of nonhomogeneous materials. *Journal of Applied Mechanics*, 67 (4), 819-822.